THE JOURNAL OF PHYSICAL CHEMISTRY A

ARTICLE

pubs.acs.org/JPCA

CASPT2 Study of the Potential Energy Surface of the HSO_2 System

Juan D. Garrido,[†,§] Maikel Y. Ballester,[‡] Yoelvis Orozco-González,[†,⊥] and Sylvio Canuto*[,†]

[†]Instituto de Física, Universidade de São Paulo, CP 66318, 05314-970 São Paulo, SP, Brazil

[‡]Departamento de Física, ICE, Universidade Federal de Juiz de Fora, MG 36036-330, Brazil

Supporting Information

ABSTRACT: The importance of the HSO_2 system in atmospheric and combustion chemistry has motivated several works dedicated to the study of associated structures and chemical reactions. Nevertheless controversy still exists in connection with the reaction $SH + O_2 \rightarrow H + SO_2$ and also related to the role of the HSOO isomers in the potential energy surface (PES). Here we report high-level ab initio calculation for the electronic ground state of the HSO_2 system. Energetic, geometric, and frequency properties for the major stationary states of the PES are reported at the same level of calculations: CASPT2/aug-cc-pV(T+d)Z. This study introduces three new stationary points (two saddle points and one minimum). These structures allow the connection of the skewed $HSOO_s$ and the HSO_2 minima defining new reaction paths for $SH + O_2 \rightarrow H + SO_2$ and $SH + O_2 \rightarrow OH + SO$. In addition, the location of the HSOO isomers in the reaction pathways have been clarified.

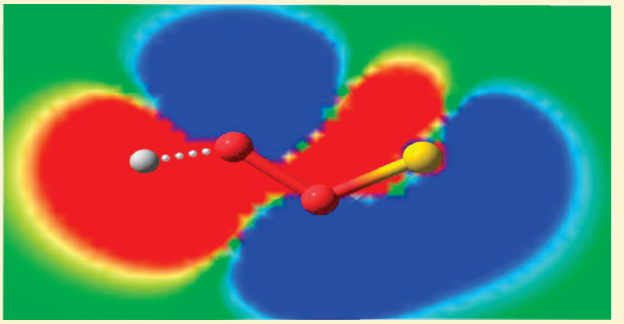

1. INTRODUCTION

Sulfur is one major contaminant in the atmosphere having significant implications in the environment. These include acid rain, air pollution, and global climate changes.[1−3] In addition, sulfur compounds have significant impact on fuel combustion processes.[4,5] In particular, isomers of HSO_2 are known to play an important role in atmospheric and combustion chemistry. To better understand the role of these compounds in these processes, a large number of theoretical and experimental studies have been performed aimed at characterizing HSO_2 isomers and the associated chemical reactions.[6−46]

According to previous theoretical studies, the potential energy surface (PES) for the electronic ground state of HSO_2 may be divided in two energetic regions; the first, named here as the lower-energy region, includes the global minimum and the asymptotic limits OH + SO and H + SO_2. The second one, which will be referred to as the upper-energy region, comprises the HOOS isomers, together with the HSO + O and HS + O_2 dissociation limits. With such a denomination we can classify the theoretical works on HSO_2 into three groups. The first group is formed by those where the purpose is the description of the lower-energy stationary points.[6−21] The second one is integrated by only a few works studying the region of the PES with higher energy,[22−24] and the third is constituted by works that have been oriented toward the description of stationary points of both regions, including connections between them.[25−31] The present work belongs to this third group. More detailed analysis of previous works will be made later. For good literature revisions, the reader is addressed to refs 21, 30, and 31.

Up to now, the general consensus is that the skewed *cis*-$HSOO_s$ is the global energy minimum of the electronic ground-state HSO_2 potential energy surface,[8,10−12,14,15,17−21,25−31] followed in increasing order of energy by the *trans*-HOSO, a transition state, and the HSO_2, a local minimum. The upper-energy region described in the literature is formed by the local minima HSOO, *cis*-HOOS, *trans*-HOOS, and the corresponding associated transition states.[22−25,28−31] The possible connections between the two mentioned energy regions are not clear up to now. Marshall and co-workers,[29] based on second-order Møller−Plesset perturbation theory calculations, have indicated that all attempts to connect the HSOO and HSO_2 isomers led to the dissociation HSO + O. Ballester and Varandas have located a transition state (TS) connecting the HSO...O van der Waals minimum with the HSO_2 radical in their global double many-body expansion potential energy surface (DMBE).[30] However Sendt and co-workers[24] have discarded such a possibility, because they could not find this transition state in calculations at the complete active space self-consisting field (CASSCF) level of theory.

A major goal of the present work is therefore to report a phenomenological, more complete, view linking the high- and low-energy regions using high-level ab initio calculations for the electronic ground state of the HSO_2 system aimed at clarifying the major stationary points corresponding to the potential energy surface for such a system, maintaining the same level of calculations to obtain optimized geometries, total energies, complete basis set (CBS) extrapolation, zero-point vibrational energies (ZPVEs), frequencies, and their intensities for all

Received: September 5, 2010
Revised: January 19, 2011
Published: February 16, 2011

identified stationary points. The paper is organized as follows. Section 2 provides a brief description of the ab initio calculations, whereas the results are presented and discussed in section 3. The major conclusions are gathered in section 4.

2. COMPUTATIONAL METHODS

The geometries, total energies, harmonic vibrational frequencies, and zero-point vibrational energies of different minima of the HSO_2 PES, and their associated transition states (TSs), and also dissociation and CBS limits for the HSO_2 system were calculated by means of the Rayleigh−Schrödinger second-order perturbation theory (CASPT2)[47−51] with reference wave functions obtained from CASSCF calculations. Full valence space was considered in the CASSCF calculations. Because of computational limitations, the number of determinants in the reference functions was kept below nine. The selection of the CASPT2 method is in accord with the purpose of a semiquantitative study and our computational limitations. This method has been recognized as having "a high computational efficiency and satisfactory accuracy".[52] Considering that the standard correlation-consistent polarized valence hierarchy (cc-pVXZ) basis sets[53,54] introduce some difficulties in predictions for sulfur systems,[55−58] we have used the Dunning's correlation consistent basis containing extra tight d functions denoted by aug-cc-pV(X+d)Z[59] for the S atom and aug-cc-pVXZ for the H and O atoms. Geometry optimizations were provided with X = T.

There are several papers devoted to the calculation of stationary points belonging to the ground state of the HSO_2 PES,[6−31] but only a few[21,23,31] reported CBS extrapolations. The very complete study of the global minimum of the PES by Wheeler and Schaefer III[21] is the only one that shows a division of the total energy in the Hartree−Fock and correlations parts, using for the Hartree−Fock (HF) energy the expression[60]

$$E_X^{\mathrm{HF}} = E_\infty + B\exp(-CX) \quad (1)$$

and for the correlation energy the two-parameter formula[61]

$$E_X^{\mathrm{cor}} = E_\infty + BX^{-3} \quad (2)$$

where E_∞, B, and C are the parameters to be fitted to the calculated energies.

In ref 23 the CBS extrapolation scheme of three parameters (1) for the total energy calculated at the PMP2/aug-cc-pVXZ level (with X = 2−4) was used. Dixon and collaborators have utilized two different approaches to extrapolate the total energy in ref 31 making use of the fact that the energy convergence is dominated by the behavior of the correlation energy. In this work several stationary points for the HSO_2 PES were calculated at the CCSD(T) level of calculation. The geometries were optimized using the aug-cc-pV(T+d)Z basis set, and then these geometries were used in single-point calculations with aug-cc-pV(D+d)Z, aug-cc-pV(Q+d)Z, and aug-cc-pV(5+d)Z basis sets. In one of the CBS extrapolations the authors of the mentioned paper have fitted energies obtained with X = 2−4 to the three-parameters expression[62]

$$E_X^{\mathrm{tot}} = E_\infty + B\exp[-(X-1)] + C[-(X-1)^2] \quad (3)$$

The data from the single X = 4−5 calculations was fitted with formula 2.

We are aware of interesting studies concerning the methods for CBS extrapolations (see ref 63 and references therein), but considering the purposes of this paper, the semiquantitative level of the employed CASPT2 method, the already mentioned dominance of the correlation energy, and the fact that the best data for comparing our results are those in ref 31, we have decided to follow the same (eq 3) CBS extrapolation method as that in ref 31. Thus, to consider the basis set superposition error (BSSE), single-point calculations were also carried out with X = D, Q (using the optimized geometries calculated with X = T) to obtain a one-electron complete basis set extrapolation.

The reactants and products connected by each transition state were confirmed by the normal mode of the imaginary frequency and following the intrinsic reaction coordinate. As starting guesses for the geometry optimizations, we have employed geometries reported previously.[24,30] To obtain the new saddle points, optimized calculations using a grid of points near the HSOO and HSO_2 minima have been provided. The rational functional approach has been used as the search algorithm for the minima, while the quadratic steepest descend method has been employed for transition state optimizations. Also the quadratic steepest descend reaction path method has been utilized to determine the reaction path (intrinsic reaction coordinates). The vibrational frequencies and ZPVE for all stationary points were computed at the same level of the theory using the program FREQUENCIES implemented in the MOLPRO.[64] The harmonic vibrational frequencies and ZPVE are reported without the consideration of any scaling factor.[65] To obtain the dissociation energies, we carried out partial optimizations keeping frozen the characteristic coordinate for the corresponding dissociation channel. To confirm the obtained values, optimized calculations of the separate fragments were also computed. All calculations in the current work were performed using the MOLPRO system of ab initio programs.[64]

3. RESULTS AND DISCUSSION

Figures 1 and 2 display absolute energy diagrams for the PES of the HSO_2 system obtained at the CASPT2/aug-cc-pV(T+d) level. The solid lines in these figures connect the reagents and products to the respective transition states. Energies in graphs (a) of these figures do not include ZPVE correction. Figures 3 and 4 show ball-and-stick drawings of the most relevant stationary points. In these figures the geometrical characteristics of these points have been indicated. Global and local minima are represented in Figure 3, while the corresponding transition states are shown in Figure 4. The arrows in this last figure indicate the displacements associated with the imaginary frequencies.

Table 1 collects calculated total energies of the stationary points and dissociation limits in the upper-energy region of the PES calculated at the CASPT2/aug-cc-pV(T+d) level. There, ZPVE values are presented in the third column. In the fourth column of Table 1, the energy of each stationary point is referred to the preceding one, while in the fifth column energies are referred to the SH + O_2 dissociation limit considering, in both cases, the ZPVE corrections. Similarly Table 2 shows energy values for the lower-energy region of the PES. In Table 3 are presented overall barriers for several reactions allowed on the PES. For comparison the table also shows results from previous authors. The values corresponding to frequencies, single-point calculations, and CBS extrapolations for all stationary points are given in the Tables 1−3 of the Supporting Information. In general the energy profile obtained with the CBS extrapolations is very similar to the one found in the raw calculations. Deviations of this behavior will be analyzed below.

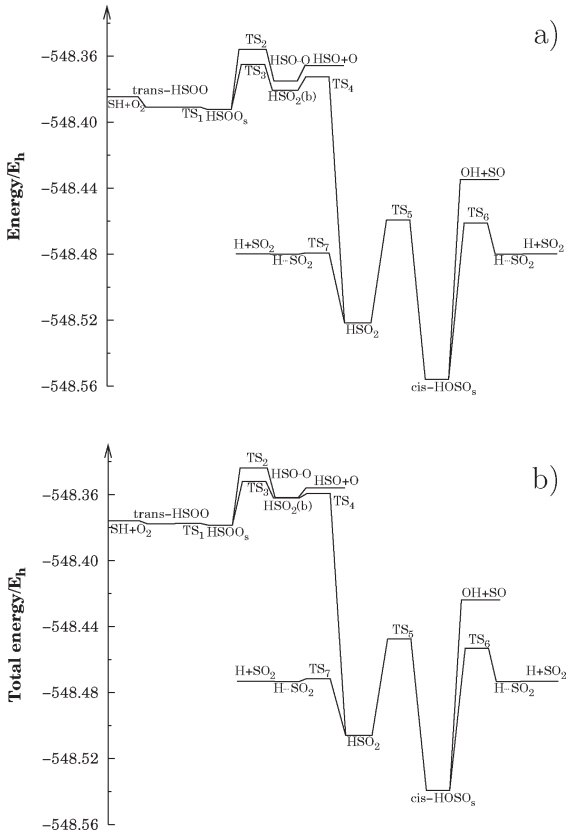

Figure 1. Ab initio potential energy surface for the SH + O_2 → HSO + O, SH + O_2 → OH + SO, and SH + O_2 → SO_2 + H reactions calculated at the CASPT2/aug-cc-pV(T+d)Z level. The ordinate represents the total energy. Results without (a) and with (b) ZPVE correction.

3.1. Pathway for Reaction SH + O_2 → O +HSO. In Figure 1 is represented the schematic potential energy diagram for the reaction SH + O_2→ O + HSO at the CASPT2 level. This reaction pathway is included in the upper-energy region of the PES. Despite that reactive pathways for the reaction have been suggested in refs 23, 24, 29, and 30 , there are some differences with our prediction. In ref 29 it was not possible to determine a TS to join the HSOO local minimum with the dissociation limit O + HSO. Sendt and collaborators[24] and Resende and Ornellas[23] reported the same transition state (TS_1) to join the $HSOO_s$ minimum with the SH + O_2 dissociation limit for both reaction SH + O_2 → O + HSO and SH + O_2 → OH + SO, whereas we have found a different situation. According to our calculations a transition state (TS_1), with C_1 symmetry, is included in the pathway for the first reaction. This transition state produces relatively low-energy barriers (and therefore small imaginary frequency) corresponding to rotations about the H−S−O−O torsional angle. These rotations convert the planar minimum *trans*-HSOO into the skewed isomer $HSOO_s$ defining an essentially barrierless process for the rotation of the H−S bond. A similar TS appears in ref 30 with a longer S−O bond (about 0.5 Å) and higher barriers with the $HSOO_s$ minimum and the SH + O_2 limit (also the reported imaginary frequency is higher). The transition states leading to a $HSOO_s$ minimum reported in refs 23and 24 will be discussed later.

Although the geometric properties of $HSOO_s$ radical shown in Figure 3, the energetic difference with *trans*-HSOO and *cis*HSOO

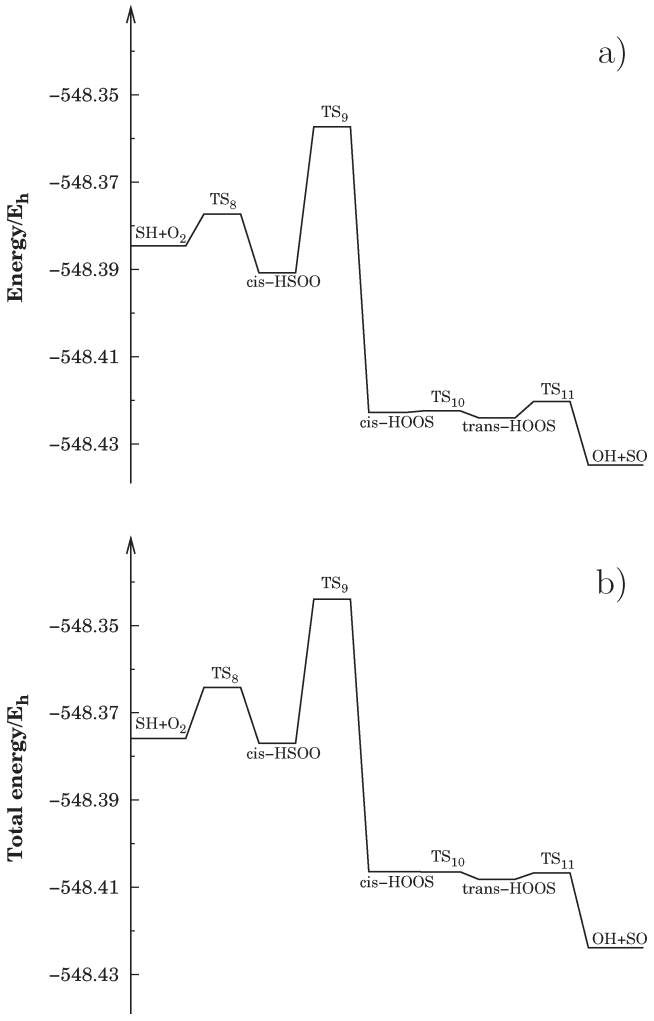

Figure 2. Ab initio potential energy suface for the SH + O_2 → OH + SO reaction calculated at the CASPT2/aug-cc-pV(T+d)Z level. The ordinate represents the total energy. Results without (a) and with (b) ZPVE correction.

isomers, and the calculated frequencies for this stationary point are in very good agreement with the recent CCSD(T)/aug-cc-pV(T+d)Z calculations of Dixon et al.[31] (differences less than 10%, 15%, and 9%, respectively), the 1.7 kcal/mol energetic difference with the SH + O_2 dissociation limit results is lower than the 7.1 kcal/mol reported in ref 31 (throughout the paper, the analysis in the text includes the ZPVE corrections for our energetic results). Also the $HSOO_t$ radical with C_s symmetry reported in the former work[31] shows properties very similar to our *trans*-HSOO minimum (differences less than 3% for geometric and frequency properties) with the exception of one particularly low imaginary frequency. Table 3 of the Supporting Information shows a comparison of the CBS extrapolation energy values for the HSOO isomers obtained in ref 31 and in this work. It is seen that in both papers very small energetic differences are obtained between these isomers (in all approaches).

The geometric characteristics of the $HSOO_s$ minimum are also very similar to those reported in refs 23−25, 28, and 30 (differences less than 7%). Energetic differences with the SH + O_2 dissociation limit of 0.90 kcal/mol in DMBE PES[30] and −0.31 kcal/mol found in ref 24 at the MRCI/aug-cc-pV(Q+d)Z level compare well with our result.

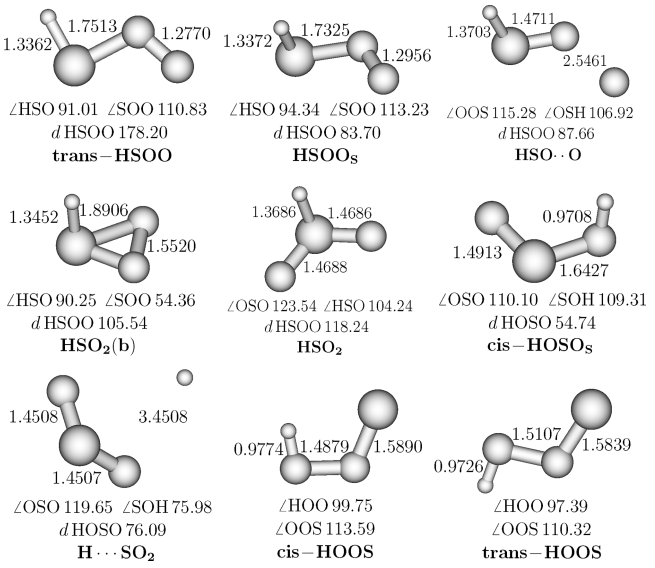

Figure 3. Ball-and-stick representation of the calculated minima corresponding to the HSO_2 potential energy surface. The geometric properties of the structures are also shown.

Along the SH + O_2→ O + HSO pathway, the $HSOO_s$ local minimum is followed by the TS_2 transition state connecting the former minimum with the HSO··O one. The double dot notation used indicates the rupture of the O−O bond because of the large distance of 2.55 Å between the two oxygen atoms. TS_2 is predicted to be above the $HSOO_s$ and HSO··O local minima by 21.8 and 11.2 kcal/mol, respectively. It shows energetic differences of +20.0 and +7.5 kcal/mol with the HS + O_2 and HSO + O dissociation limits. Therefore, our results confirm the consensus that the formation of HSO + O is an endothermic process. The barriers obtained for TS_2 in the CBS extrapolation (see Table 3 in the Supporting Information) result are too high as a result of the value appearing in the single-point calculation with the aug-cc-pV(Q+d) basis set for this TS. It could mean that there exists some differences in the optimized geometries for the aug-cc-pV(T+d) and aug-cc-pV(Q+d) basis sets.

The mentioned structures have also been reported by previously.[24,30] Although the geometric properties of the TS reported in ref 24 are similar to those of the TS_2 (differences less than 6%), the indicated frequencies show larger differences, especially for the imaginary one (a difference of about 45%). Also, their energetic separation with respect to the $HSOO_s$ minimum of 19.3 and 21.5 kcal/mol obtained at the CASSCF and MRCI levels is consistent with our results, while the 3.7 and 0.11 kcal/mol reverse barriers are lower than the corresponding ones reported here. Note that they[24] have obtained the van der Waals minimum using a partially optimized procedure leading to a minimum near the dissociation limit HSO + O, while we have provided a full optimization of the mentioned HSO··O local minimum. The geometrical concordance with the corresponding TS in ref 30 is better than 10% for any parameter, and the frequencies are also similar. The energetic difference with the HSO··O minimum of 7.2 kcal/mol is not quite different from our result; however, the forward barrier of 8.4 kcal/mol and the energetic gap of 9.3 kcal/mol with the SH + O_2 limit differ substantially from our calculated values.

3.2. Pathways for Reactions SH + O_2→ OH + SO (Lower-Energy Region), SH + O_2→ H + SO_2, and OH + SO → H + SO_2. Figure 1 shows a pathway for OH + SO formation containing the most stable stationary point of the HSO_2 PES. In this scheme the $HSOO_s$ and HSO_2 local minima are connected by the TS_3 transition state and the HSO_2 (b) minimum (both with C_1 symmetry) and the TS_4 saddle point (with C_s symmetry). The normal mode of the imaginary vibration in the TS_3 transition state is oriented to produce the approximation of final oxygen atom in the S−O−O chain to the sulfur atom until the formation of the bonded HSO_2 (b) structure. In the next step the vibrations of the O−O bond in the TS_4 saddle point lead to formation of the unbounded HSO_2 local minimum with C_s symmetry (see Figure 3).

The TS_3 transition state shows energetic barriers of 16.8 and 6.4 kcal/mol with $HSOO_s$ and HSO_2 (b), while the TS_4 has energetic differences of 1.7 and 92.0 kcal/mol with the HSO_2 (b) and the HSO_2 local minima. The negative frequencies of both transition states have relative intensities of 100%. These structures have not been reported before.

The small energetic difference between the HSO_2 (b) local minimum and the TS_4 and the inverted order for the energies of these stationary points obtained in the CBS extrapolation (see Table 2 in the Supporting Information) led us to conclude that this region of the PES requires even more accurate calculations using a more dense grid of points in the vicinity of both stationary points.

Although a transition state connecting the HSO···O and HSO_2 stationary points was indicated in the DMBE PES of ref 30, the attempts to verify its existence at both the CASSCF/aug-cc-pVDZ level in ref 24 and in this present work at the CASPT2 level indicate that the mentioned structure is not a saddle point. In the same paper[24] the authors mention that their efforts to locate a transition state leading to the formation of HSO_2 from the reactants SH + O_2 were unproductive. A similar conclusion is reported in refs 23 and 29.

The low part of the reaction path in Figure 1 includes the well-studied HSO_2 and HOSO structures. The HOSO radical has three isomers: *cis*-HOSO and *trans*-HOSO with a plane geometry and the skewed *cis*-$HOSO_s$ (C_1 symmetry). Several papers have been devoted to the study of the HOSO structure, both theoretically and experimentally.[6,8−12,14−16,18−21,26−28,30,31] Very recently, two very extensive theoretical studies have appeared[21,31] where it was demonstrated that the *cis*-$HOSO_s$ isomer is the most stable. In this work we have focused our attention on the *cis*-$HOSO_s$ and *trans*-HOSO isomers. The geometrical properties (within 2%) and frequencies (with differences around 7% with the exception of the imaginary one that shows a difference of about 30%) calculated by us at the CASPT2 level are in excellent agreement with the mentioned papers.[21,31] Only the dihedral angle for the *cis*-$HOSO_s$ isomer is larger than the one obtained in ref 21 (54.7° vs 24.2°). The energetic difference between these isomers is also in excellent accord (2.0 vs 2.3 kcal/mol in ref 21). Frequencies for three vibrational modes of the *cis*-HOSO in solid matrix of Ar, Kr, and Xe were reported in ref 15. The frequencies measured in Ar matrix differ by 1, 63, and 196 cm^{-1} for the two SO stretch and the OH stretch modes obtained here, respectively.

According to our present calculations, the energetic level of the *cis*-$HOSO_s$ global minimum is 41.6, 72.5, and 102.6 kcal/mol lower than the H + SO_2, OH + SO, and SH + O_2 dissociation limits, respectively; these values are in excellent agreement with the 44.2, 71.8, and 96.0 kcal/mol reported in ref 30; also, the 69.1 calculated in ref 31 with the OH + SO limit is in good

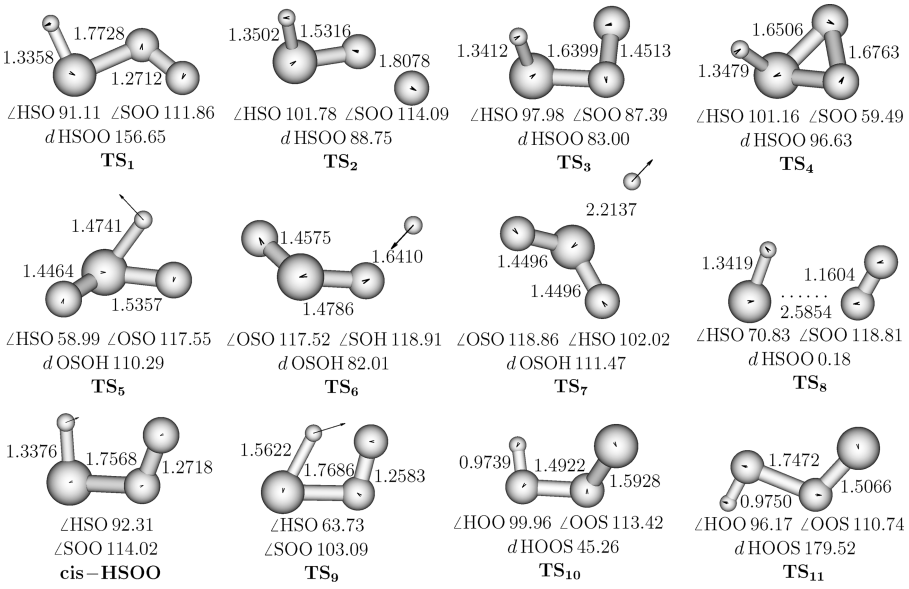

Figure 4. Ball-and-stick representation of the calculated transition states corresponding to the HSO_2 potential energy surface. The geometric properties of the structures are also shown. The arrows indicate the displacements associated with the imaginary frequencies.

Table 1. Energetic Properties for Stationary Points in the Upper-Energy Region of the HSO_2 PES

stationary point	total energy (au)	ZPVE (au)	difference with previous stationary point (kcal/mol)	difference with the SH + O_2 limit (kcal/mol).
			HS + O_2 → OH + SO Reaction Pathway	
HS + O_2	−548.38457423	0.00872692	0.0	0.0
TS_8	−548.37729620	0.01313236	+7.3	+7.3
cis-HSOO	−548.39078414	0.01382676	−8.0	−0.7
TS_9	−548.35732700	0.01337374	+20.7	+20.0
cis-HOOS	−548.42283775	0.01641262	−39.2	−19.2
TS_{10}	−548.42242142	0.01599226	0.0	−19.2
trans-HOOS	−548.42397423	0.01583925	−1.1	−20.3
TS_{11}	−548.42032895	0.01361613	+0.9	−19.4
OH + ^{3}SO	−548.43485120	0.0109856	−10.8	−30.1
			HS + O_2 → O + HSO Reaction Pathway	
$HSOO_s$	−548.39242944	0.01382676	−0.7	−1.7
TS_2	−548.35589262	0.01198362	+21.8	+20.0
O...HSO	−548.37507429	0.01337365	−11.2	+8.9
O + HSO	−548.36569340	0.00984816	+3.7	+12.6

concordance. In relation with the $HSOO_s$ local minimum, our global minimum is about 15% deeper with respect to calculations in ref 31.

At the CASPT2 level two reaction paths allow for the formation of H + SO_2 from SH + O_2 reactants. In both cases the dissociation limit is preceded by the H···SO_2 van der Waals complex energetically separated from the former by 0.2 kcal/mol. In the first pathway the TS_6 transition state (where imaginary vibration separates the final hydrogen of the O−S−O chain) connects directly the global minimum *cis*-$HOSO_s$ with the van der Waals complex. In the second one, the imaginary mode of the TS_7 transition state moves the hydrogen atom until breaking its bond with the sulfur in the HSO_2 minimum. These mechanisms are also exothermic and warrant the H + SO_2 formation from OH + SO.

Despite the mentioned disagreement with the PES obtained using DMBE[30] in relation to the transition state connecting with the stationary point HSO_2 (note that, although the geometries of HSO···O and HSO_2 (b) do not match, the energy difference between them is a very small value of 0.2 kcal/mol), we should notice that qualitatively the general picture in the low region of Figure 1 is indeed similar to the equivalent diagram in ref 30, with the exception of the TS_7, not reported there. Although the geometric properties of TS_5 agree with the similar transition state reported in ref 30 (differences less than 4% with the exception of dihedral angle with difference of 44%), it has lower energy barriers by about 13 kcal/mol and the frequencies show more substantial differences. The TS_6 saddle point compares well with the equivalent transition state in this paper[30] (better than 4%), but frequencies show differences of about 50% .

In ref 14 a B3LYP/6-31+G(d) PES for the reaction OH + SO → H + SO_2 that is very similar to the low part of Figure 1was reported. Only the H···SO_2 minimum is not included there.

Table 2. Energetics of the Stationary Points in the Lower-Energy Region of the HSO_2 PES

stationary point	total energy (au)	ZPVE (au)	difference with previous stationary point (kcal/mol)	difference with the SH + O_2 limit (kcal/mol)
			HS + O_2 → OH + SO Reaction Pathway	
HS + O_2	−548.38457423	0.00872692	0.0	0.0
trans-HSOO	−548.39091723	0.01332704	−1.1	−1.1
TS_1	−548.39088689	0.01335814	+0.0	−1.1
$HSOO_s$	−548.39242944	0.01382676	−0.7	−1.7
TS_3	−548.36518342	0.01328699	+16.8	+15.0
HSO_2 (b)	−548.38064416	0.01855706	−6.4	+8.6
TS_4	−548.37262674	0.01330662	+1.7	+10.4
HSO_2	−548.52165409	0.01568766	−92.0	−81.7
TS_5	−548.45949288	0.01195595	+36.7	−45.0
cis-$HOSO_s$	−548.55599064	0.01658146	−57.7	−102.6
OH + ^{3}SO	−548.4348512	0.01098560	+72.5	−30.1
			HS + O_2 → H + SO_2 Reaction Pathway (1)	
cis-$HOSO_s$	−548.55599064	0.01658146	−57.7	−102.6
TS_6	−548.46125675	0.00814027	+54.2	−48.5
H...SO_2	−548.48006774	0.00673368	−12.7	−61.2
H + SO_2	−548.47980364	0.00673750	+0.2	−61.0
			HS + O_2 → H + SO_2 Reaction Pathway (2)	
HSO_2	−548.52165409	0.01568766	−92.0	−81.7
TS_7	−548.47928308	0.00777670	+21.6	−60.0
H...SO_2	−548.48006774	0.00673368	−1.2	−61.2
H + SO_2	−548.47980364	0.00673750	+0.2	−61.0

Table 3. Overall Barriers (kcal/mol) for Indicated Chemical Reactions

		overall barrier			
reaction	TS	this work	[30] DMBE	[24] MRCI	[23] CCSD(T)
SH+O_2 → HSO + O	TS_2	20.0	21.7[a]	21.2	22.6*
SH+O_2 → SO + OH (lower-energy region)	TS_3	15.0	9.3	–	–
SH+O_2 → SO + OH (upper-energy region)	TS_9	20.0	–	19.4	33.0
SH+O_2 → H + SO_2	TS_3	15.0	9.3	–	–

[a] These values are the difference between the dissociation limits. The energetic values in the table consider the ZPVE corrections.

However, geometries of the stationary points and energetic differences between OH + SO and H + SO_2 dissociation limit reported in the cited paper fit quite well with our results; the barriers of the saddle points are below about 10 kcal/mol.

3.3. Pathway for Reaction SH + O_2 → OH + SO (Upper-Energy Region). Figure 2 schematically represents the calculated potential energy diagram for the reaction SH + O_2→ OH + SO. In this case the reaction follows a pathway included in the upper-energy region of the PES. For the formation of the *cis*-HSOO stationary point (with C_s symmetry), a transition state TS_8 with barrier heights of 7.3 and 8.0 kcal/mol for the forward and reverse processes, respectively, was found at the CASPT2 level. The reverse barrier height is in excellent agreement with the MP4/6-311G(d,p) calculation in refs 25 and 29 (9.3 kcal/mol). The forward barrier height is less than the 12.9 kcal/mol value reported in ref 23 at the multireference MP2(9,10) level. Note that the approach of the SH diatom to the oxygen molecule following a planar geometry with parallel position of diatomic axes has a higher energetic barrier than the approximation in an antiparallel position with some torsional displacement of the axes.

The *cis*-HSOO isomer was also reported in ref 31 with basically the same geometry, frequencies, and energetic difference with the $HSOO_s$ local minimum (about 1.0 kcal/mol more stable). But we obtain a lower imaginary frequency (120 cm^{-1} by 81 cm^{-1}).

Our minimum energy reaction path calculations show that this transition state produces essentially no barrier to rotation of the H−S bond to convert the $HSOO_s$ minimum (with dihedral angle of +83.7°), into its mirror symmetric isomer (with dihedral angle of −83.7°). The relatively low intensity of the imaginary vibration and the very small energetic difference between the *cis*-HSOO and $HSOO_s$ isomers make possible the connection of TS_8 and TS_9 through the *cis*-HSOO radical. This prediction could be verified by dynamics calculations.

In a CASSCF study of the SH + O_2→ OH + SO reaction (included in the upper-energy region), Sendt and co-workers[24] introduced a reaction pathway where the SH + O_2 dissociation limit is joined to the $HSOO_s$ local minimum by a transition state with geometric properties quite similar to our TS_1 transition state (with the exception of the dihedral angle of 76.5° vs our 156.6°).

In the same paper the authors provide single-point energy calculations at the MRCI level using CASSCF geometries and led to the conclusion that the formation of $HSOO_s$ is a barrierless process (0.66 kcal/mol).[24] A similar result was obtained in ref 29 with calculations at the MP2/6-31G(d) and G2 levels. Figure 1 also shows extremely small energetic difference between *trans*-HSOO, TS_1, and $HSOO_s$ isomer (less than 1 kcal/mol), at the CASPT2 level of calculation, but the minimum energy reaction path shows that the $HSOO_s$ local minimum connects, in fact, with TS_1, TS_2, and TS_3 transition states in other reaction pathways, as already discussed above. According to our calculations, in the upper-energy region the products OH + SO are connected with the reactants by the TS_8 transition state and the *cis*-HSOO local minimum.

Although in the CASPT2/aug-cc-pV(T+d)Z level the calculations of the reaction path led to the situation described before, the very small energetic difference between the three isomers of the HSOO structure indicates that they have essentially the same statistical weight and should thus have the same importance from the chemical reactive point of view.

In Figure 2 is seen a transition state (TS_9) with C_s symmetry connecting the stationary points *cis*-HSOO and *cis*-HOOS with forward and reverse barriers of 20.71 and 39.20 kcal/mol, respectively. Goumri et al.[29] could not locate a TS for the HOOS → HSOO isomerization at the MP2/6-31G(d) level. In the DMBE PES by Ballester and Varandas,[30] this SH + O_2 → OH + SO path, in the upper-energy region, is not reported. Reference 23 presented a pathway for the indicated reaction at the multireference MP2 level of theory where the *trans*-HOOS isomer does not appear. There it was indicated that at the multireference MP2 level the *cis*-HOOS is not a stable species, and it was then considered to be a false minimum. However, Resende and Ornellas[23] report a TS_2 with a C_1 symmetry connecting the $HSOO_s$ minimum directly to the products SO + OH with reverse and forward barriers at the CCSD(T)/CBS level of 54.8 kcal/mol (in good agreement with our value of 50.2 kcal/mol with the SO + OH dissociation limit) and 37.2 kcal/mol (16.5 kcal/mol above our result), respectively. Sendt and co-workers[24] report a similar plane transition state (geometric differences less than 10%) at the full valence CASSCF/cc-pVTZ level of theory for geometry optimization. The energetic barriers of this transition state at the same level of theory are 30.9 kcal/mol (with a difference of 33% with our present result) and 33.7 kcal/mol (in good agreement with our above-mentioned result). However the single-point energy calculations at the MRCI+Davidson/aug-cc-pV(Q+d)Z level of theory using the calculated CASSCF geometries reported in this paper remarkably reduce these differences (they obtained 19.7 and 34.3 kcal/mol for the barriers with this approximation). Note that the energetic difference of 18.5 kcal/mol between the $HSOO_s$ and *cis*-HOOS minima obtained here compares well with the corresponding value of 15.0 kcal/mol calculated by Dixon et al.[31] (19.3 and 15.2 kcal/mol, respectively, in the CBS limit). The values obtained by Marshall and co-workers[25] (10.9 kcal/mol) compared with the *trans*-HOOS and the difference of 12.2 kcal/mol reported by Frank et al.[28] for the enthalpies of *cis*-$HOOS_s$ and *cis*-$HSOO_s$ are not far from our results.

Figure 2 also shows a reaction path after the TS_9 transition state constituted by the *cis*-HOOS and *trans*-HOOS minimums (both with C_s symmetry) connected by the TS_{10} transition state. At the end of the path a transition state (the TS_{11}) joins the *trans*-HOOS minimum with the SO + OH dissociation limit. Geometries of all these stationary points are very close to those reported in refs 24and 31. Note that the inclusion of the ZPVE correction leads to the location of the TS_{10} saddle point slightly below the *cis*-HOOS minimum at the CASPT2/aug-cc-pV(T+D)Z level. However the CBS extrapolations show the *cis*-HOOS isomer below the transition state. These results suggest the necessity of a higher level of calculation for a better qualitative and quantitative description of these stationary points. The extremely small energetic differences between these structures reported in Table 3 suggest a rapid transit from the *cis*-HSOO isomer through these structures to the OH + SO dissociation limit after passing over the barrier of the TS_9 transition state. The same conclusion was obtained in refs 23 and 24.

3.4. Overall Barriers for Reactions with Reactants SH + O_2. Table 3 presents the overall barriers for reactions allowed by the calculated PES when the reactants are the diatoms SH and O_2. This table also includes data reported by other authors. The first interesting aspect that emerges from this table is that the formation of H + SO_2 and OH + SO, following the reaction paths included in the lower-energy region, is energetically more favorable. The second is that barriers for the products O + HSO and OH + SO, following the reaction pathways included in the upper-energy region, are basically equivalent. Thus, these processes are energetically competitive. This, together with the form of the reaction pathways in Figures 1 and 2, suggests than for total energy values below the barriers of TS_2 and TS_9 and above TS_3 the dominant process should be the formation of the H + SO_2 products. But above TS_2 and TS_9, the form of the minimum energy reaction paths suggests the possible dominant formation of O + HSO and OH + SO (following the path in Figure 2), because the lower paths require more structural rearrangements. As it was mentioned above, in ref 30 appears a different transition state to connect the lower- and upper-energy regions. This fact produces the differences shown in Table 3.

4. CONCLUSIONS

An ab initio potential energy surface, at the CASPT2/aug-cc-pV(T+D)Z level of theory, has been reported for the ground electronic state of the HSO_2 tetra-atomic system. The properties of the stationary points obtained here are, in general, in good agreement with previously reported theoretical results. But now a new path connecting the upper-energy and lower-energy regions of the PES is reported. This path joins the $HSOO_s$ and HSO_2 local minima through the new TS_3 and TS_4 transition states and the HSO_2 (b) local minimum, and it makes possible the reaction SH + O_2 → H + SO_2. In this more complete study of HSOO isomers, it was shown how they are connected with the other structures of the PES. The characterization of the *cis*-$HOSO_s$ global minimum is in good agreement with the available experimental data. Furthermore, the present work predicts the energetic interval for dominant production of H + SO_2 and O + HSO from HS + O_2. This proposition could be verified experimentally. The results obtained in this paper could be used to improve the DMBE PES published in ref 30. Of course a final evaluation of the presented results requires new experimental data and dynamics studies of the various chemical reactions allowed by the PES.

■ ASSOCIATED CONTENT

Supporting Information. Vibration frequencies and relative intensities for all stationary points of the HSO_2 PES; CASPT2/aug-cc-pV(X+d)Z energies with X = D, T, and Q in

atomic units; CBS extrapolation energies in atomic units and difference with previous stationary point (in kcal/mol); comparison of the energetic differences between stationary points according to ref 31 and this work (in kcal/mol). This material is available free of charge via the Internet at http://pubs.acs.org.

AUTHOR INFORMATION

Corresponding Author

*E-mail canuto@if.usp.br.

Present Addresses

[§]Universidad Politécnica Metropolitana de Hidalgo, Col. Morelos, Pachuca de Soto, C.P. 42040, Hidalgo, México.

[⊥]Grupo de Modelación, Centro de Estudios Ambientales de Cienfuegos (CEAC), Ciudad Nuclear, Cienfuegos, Cuba.

ACKNOWLEDGMENT

This work has been partially supported by CNPq and FAPESP. J.D.G., in particular, thanks FAPESP for a visiting professor scholarship.

We thank Prof. Benedito J. C. Cabral and Marco Antonio Chaer Nascimento for discussions and computational facilities in Lisbon and Rio de Janeiro.

REFERENCES

(1) Wayne, R. P. *Chemistry of Atmospheres*; Oxford University Press: New York, 2002.

(2) Finlayson-Pitts, B. J.; Pitts, J. N., Jr. *Chemistry of the Upper and Lower Atmosphere*; Academic Press: San Diego, CA, 2000.

(3) Warneck, P. *Chemistry of the Natural Atmospheres*: Academic Press: New York, 1988.

(4) Arutyunov, V. A.; Vedeneev, V. I.; Ushakov, V. A.; Shumova, V. V. *Kinet. Katal.* **1990**, *31*, 6.

(5) Glarborg, P. *Proc. Combust. Inst.* **2007**, *31*, 77–98.

(6) Boyd, R. J.; Gupta, A.; Langler, R. F.; Lownie, S. P.; Pincock, J. A. *Can. J. Chem.* **1980**, *58*, 331–338.

(7) Hinchliffe, A. *J. Mol. Struct.* **1981**, *71*, 349–352.

(8) Binns, D.; Marshall, P. *J. Chem. Phys.* **1991**, *95*, 4940–4947.

(9) Laakso, D.; Marshall, P. *J. Chem. Phys.* **1992**, *96*, 2471–2474.

(10) Qi, J.-X.; Deng, W.-Q.; Han, K.-L.; He, G.-Z. *J. Chem. Soc., Faraday Trans.* **1997**, *93*, 25–28.

(11) Drozdova, Y.; Steudel, R.; Hertwig, R. H.; Koch, W.; Steiger, T. *J. Phys. Chem. A* **1998**, *102*, 990–996.

(12) Isoniemi, E.; Khriachtchev, L.; Lundell, J.; Räsänen, M. *J. Mol. Struct.* **2001**, *563−564*, 261–265.

(13) Denis, P. A.; Ventura, O. N. *Chem. Phys. Lett.* **2001**, *344*, 221–228.

(14) McKee, M. L.; Wine, P. H. *J. Am. Chem. Soc.* **2001**, *123*, 2344–2353.

(15) Isoniemi, E.; Khriachtchev, L.; Lundell, J.; Räsänen, M. *Phys. Chem. Chem. Phys.* **2002**, *4*, 1549–1554.

(16) Wang, L.; Zhang, J. *J. Mol. Struct. (THEOCHEM)* **2002**, *581*, 129–138.

(17) Wang, B.; Hou, H. *Chem. Phys. Lett.* **2005**, *410*, 235–241.

(18) Napolion, B.; Watts, J. D. *Chem. Phys. Lett.* **2006**, *421*, 562–565.

(19) Wierzejewska, M.; Olbert-Majkut, A. *J. Phys. Chem. A* **2007**, *111*, 2790–2796.

(20) Midey, A. J.; Viggiano, A. A. *J. Phys. Chem. A* **2007**, *111*, 1852–1859.

(21) Wheeler, S. E.; Schaefer, H. F., III. *J. Phys. Chem. A* **2009**, *113*, 6779–6788.

(22) Goumri, A.; Rocha, J.-D. R.; Marshall, P. *J. Phys. Chem.* **1995**, *99*, 10834–10836.

(23) Resende, S. M.; Ornellas, F. R. *Phys. Chem. Chem. Phys.* **2003**, *5*, 4617–4621.

(24) Zhou, Ch. R.; Sendt, K. B.; Haynes, S. *J. Phys. Chem. A* **2009**, *113*, 2975–2981.

(25) Laakso, D.; Smith, C. E.; Goumri, A.; Rocha, J.-D. R.; Marshall, P. *Chem. Phys. Lett.* **1994**, *227*, 377–383.

(26) Morris, V. R.; Jackson, W. M. *Chem. Phys. Lett.* **1994**, *223*, 445–451.

(27) Frank, A. J.; Sadílek, M.; Ferrier, J. G.; Tureček, F. *J. Am. Chem. Soc.* **1996**, *118*, 11321–11322.

(28) Frank, A. J.; Sadílek, M.; Ferrier, J. G.; Tureček, F. *J. Am. Chem. Soc.* **1997**, *119*, 12343–12353.

(29) Goumri, A.; Rocha, J.-D. R.; Laakso, D.; Smith, C. E.; Marshall, P. *J. Phys. Chem. A* **1999**, *103*, 11328–11335.

(30) Ballester, M. Y.; Varandas, A. J. C. *Phys. Chem. Chem. Phys.* **2005**, *7*, 2305–2317.

(31) Grant, D. J.; Dixon, D. A.; Francisco, J. S.; Feller, D.; Peterson, K. A. *J. Phys. Chem. A* **2009**, *113*, 11343–11353.

(32) Fair, R. W.; Thrush, B. A. *Trans. Faraday Soc.* **1969**, *65*, 1550–1556.

(33) Blitz, M. A.; Hughes, K. J.; Pilling, M. J.; Robertson, S. *J. Phys. Chem. A* **2006**, *110*, 2996–3009.

(34) Blitz, M. A.; McKee, K. W.; Pilling, M. J. *Proc. Combust. Inst.* **2000**, *28*, 2491–2497.

(35) Morris, V. R.; Han, K.-L.; Jackson, W. M. *J. Phys. Chem.* **1995**, *99*, 10086–10091.

(36) Stachnik, R. A.; Molina, M. J. *J. Phys. Chem.* **1987**, *91*, 4603–4606.

(37) Cerru, F. G.; Kronenburg, A.; Lindstedt, R. P. *Proc. Combust. Inst.* **2005**, *30*, 1227–1235.

(38) Tsuchiya, K.; Kamiya, K.; Matsui, H. *Int. J. Chem. Kinet.* **1997**, *29*, 57–66.

(39) Ballester, M. Y.; Caridade, P. J. S. B.; Varandas, A. J. C. *Chem. Phys. Lett.* **2007**, *439*, 301–307.

(40) Alzueta, M. U.; Bilbao, R.; Glarborg, P. *Combust. Flame* **2001**, *127*, 2234–2251.

(41) Ballester, M. Y.; Varandas, A. J. C. *Chem. Phys. Lett.* **2007**, *433*, 279–285.

(42) Ballester, M. Y.; Guerrero, Y. O.; Garrido, J. D. *Int. J. Quantum Chem.* **2008**, *108*, 1705–1713.

(43) Ballester, M. Y.; Varandas, A. J. C. *Int. J. Chem. Kinet.* **2008**, *40*, 533–541.

(44) Garrido, J. D.; Nascimento, M. A. C.; Ballester, M. Y. *Int. J. Quantum Chem.* **2010**, *110*, 549–557.

(45) Schofield, K. *J. Phys. Chem. Ref. Data* **1973**, *2*, 25–85.

(46) Ballester, M. Y.; Orozo-González, Y.; Garrido, J. D.; Dos Santos, H. F. *J. Chem. Phys.* **2010**, *132*, 044310–044310-6.

(47) Roos, B. O.; Linse, P.; Siegbahn, P. E. M.; Blomberg, M. R. A. *Chem. Phys.* **1982**, *66*, 197–207.

(48) Andersson, K.; Malmqvist, P.-A.; Ross, B. O.; Sadlej, A. J.; Wolinski, K. *J. Phys. Chem.* **1990**, *94*, 5483–5488.

(49) Andersson, K.; Malmqvist, P.-A.; Ross, B. O. *J. Phys. Chem.* **1992**, *96*, 1218–1226.

(50) Werner, H.-J. *Mol. Phys.* **1996**, *89*, 645–661.

(51) Celani, P.; Werner, H.-J. *J. Chem. Phys.* **2000**, *112*, 5546–5557.

(52) Bokarev, S. I.; Dolgov, E. K.; Bataev, V. A.; Godunov, I. A. *Int. J. Quantum Chem.* **2009**, *109*, 569–585.

(53) Dunning, T. H., Jr. *J. Chem. Phys.* **1989**, *90*, 1007–1023.

(54) Kendall, R. A.; Dunning, T. H., Jr.; Harrison, R. J. *J. Chem. Phys.* **1992**, *96*, 6796–6806.

(55) Martin, J. M. L. *J. Chem. Phys.* **1998**, *108*, 2791–2800.

(56) Martin, J. M. L.; Uzan, O. *Chem. Phys. Lett.* **1998**, *282*, 16–24.

(57) Bauschlicher, C. W., Jr.; Ricca, A. *J. Phys. Chem.* **1998**, *102*, 8044–8050.

(58) Bauschlicher, C. W., Jr.; Partridge, H. *Chem. Phys. Lett.* **1995**, *240*, 533–540.

(59) Dunning, T. H., Jr.; Peterson, K. A.; Wilson, A. K. *J. Chem. Phys.* **2001**, *114*, 9244–9253.

(60) Feller, D. A. *J. Chem. Phys.* **1993**, *98*, 7059–7071. Woon, D. E.; Dunning, T. H., Jr. *J. Chem. Phys.* **1993**, *99*, 1914–1929. Feller, D. A.; Peterson, K. A. *J. Chem. Phys.* **1998**, *108*, 154–176.

(61) Helgaker, T.; Klopper, W.; Koch, H.; Noga, J. *J. Chem. Phys.* **1997**, *106*, 9639–9646.
(62) Peterson, K. A.; Woon, D. E.; Dunning, T. H., Jr. *J. Chem. Phys.* **1993**, *100*, 7410–7415.
(63) Varandas, A. J. C. *J. Phys. Chem. A* **2010**, *114*, 8505–8516. Li, Y. Q.; Varandas, A. J. C. *J. Phys. Chem. A* **2010**, *114*, 9644. Varandas, A. J. C. *J. Chem. Phys.* **2007**, 244105-1–244105-15.
(64) Werner, H.-J.; Knowles, P. J.; Lindh, R.; Manby, F. R.; Schütz, M.; Celani, P.; Korona, T.; Rauhut, G.; Amos, R. D.; Bernhardsson, A.; Berning, A.; Cooper, D. L.; Deegan, M. J. O.; Dobbyn, A. J.; Eckert, F.; Hampel, C.; Hetzer, G.; Lloyd, A. W.; McNicholas, S. J., Meyer, W.; Mura, M. E.; Nicklass, A.; Palmieri, P.; Pitzer, R.; Schumann, U.; Stoll, H.; Stone, A. J.; Tarroni, R.; Thorsteinsson, T. MOLPRO, version 2009.1, a package of ab initio programs, Universität Stüttgart, Stüttgart, Germany, and University of Birmingham, Birmingham, United Kingdom; see <http://www.molpro.net>. Celani, P.; Werner, H.-J. *J. Chem. Phys.* **2003**, *119*, 5044–5057. Sun, J.; Ruedenberg, K. *J. Chem. Phys.* **1993**, *99*, 5257–5268. Sun, J.; Ruedenberg, K. *J. Chem. Phys.* **1993**, *99*, 5269–5275. Sun, J.; Ruedenberg, K. *J. Chem. Phys.* **1994**, *101*, 2157–2167. Eckert, F.; Werner, H.-J. *Theor. Chem. Acc.* **1998**, *100*, 21–30.
(65) Sendt, K.; Haynes, B. S. *Proc. Combust. Inst.* **2007**, *31*, 257–265.